

INFLUENCE OF PLASTIC DEFORMATION OF ADHEREND MATERIAL ON STRESS DISTRIBUTION IN ADHESIVE LAP JOINTS

Krzysztof Zielecki¹⁾, Lucjan Witek^{2)*}, Feliks Stachowicz³⁾

¹⁾ ZF Friedrichshafen AG, Schweinfurt, Germany

²⁾ Rzeszów University of Technology, Department of Aircraft and Aero Engines, Rzeszów, Poland

³⁾ Rzeszów University of Technology, Department of Material Forming and Processing, Rzeszów, Poland

Received: 11.10.2017

Accepted: 15.11.2017

*Corresponding author: e-mail: lwitek@prz.edu.pl; Tel.: +48-17-8651324, 12 Powstańców Warszawy Ave., 35-959 Rzeszów, Poland

Abstract

In the stress analysis of adhesive lap joints, the linear-elastic model of adherend material is often used. In some cases, when the joined material has a low yield stress, this assumption causes errors in the stress estimation in the adhesive layer or adherend. In this study, the results of numerical stress and strain analysis of adhesive lap joint were presented. In the performed analysis, both the elastic-plastic and linear-elastic models of joined materials were considered. In the first part of the study, the properties of adherend material were determined in experimental investigations. Next, the discrete model of joint was created. The results of nonlinear finite element analysis showed that for joints of materials with a low value of yield stress the plastic deformation begins in adherend at load 50% lower than destructive force of the joint. As a result of this phenomenon, the rapid stress increase in the adhesive layer is observed in an advanced phase of loading. This causes a significant decrease in strength in the lap joints of elastic-plastic materials.

Keywords: plastic deformation, stress analysis, adhesive lap joint, finite element method

1 Introduction

The adhesive joints are often used in aerospace and automotive industry. The advantage of adhesive joints is continuous load transfer without stress concentrations in comparison to welded, projection welded or riveted joints. Adhesive joints can transfer loads lower than above mentioned [1], but in some cases, there is only the one option (for example in case of necessity of joining very thin materials). Another example of the application of adhesive bonding would be joining of different materials, which cannot be welded [2-4]. Damping properties of adhesive joints might also be considered as an advantage [5]. Designers work continuously in order to increase the strength of adhesive joints. The approach to increase the strength of bonded joints is decreasing of joint stiffness in the external area of overlap by changing the geometrical parameters [6-10]. An engineering tool which allows the stress, strain and fatigue analysis of adhesive joints in engineering applications is finite element method (FEM) or boundary element method (BEM) [11-18]. Most of the research works are related to the analysis of joints with the linear-elastic material of adherend. In paper [19] the results of stress analysis of adhesive lap

joint of an elastic-plastic material were presented. The attention of work [19] was focused on both the Huber-Mises stress distribution of joint components and the maximum principal stress values in the adhesive layer.

The main objective of this study is a numerical determination of stress and plastic strain in the adhesive lap joint with an elastic-plastic model of adherend material. The attention in this study is focused on tearing (S22) stress distribution in the adhesive layer. This stress component has a large influence on the strength of adhesive lap joints.

2 Experimental material tests of adhered material and adhesive

The adhesive lap joints were made using the Araldite 2014-1 adhesive (Huntsman Advanced Materials GmbH Company). Araldite 2014-1 is two component epoxy adhesive used for connection of metal structures. The adhesive is delivered in two containers (adhesive and hardener, proportion 2:1). The adhesive was mixed using a screw mixing nozzle. In order to determine the mechanical properties of the Araldite 2014-1 adhesive, the flat specimens with the use of casting method were first prepared. The specimens were next tensioned in the static test. The results of tension tests performed for two specimens are presented in **Fig. 1**. On the base of performed experimental investigations the following mechanical properties of Araldite 2014-1 adhesive were determined: Young's modulus $E = 3425$ MPa, and ultimate tensile strength $UTS = 21.8$ MPa. Obtained results (**Fig. 1**) show that Araldite 2014-1 adhesive after hardening can be considered as linear-elastic material.

The joined sheets were made of S185 low-carbon steel [20]. The tension test of S185 steel (plot of stress vs strain) does not take into account the cross-section changes during the tension of the specimen. In order to define the elastic-plastic model of material (according to Abaqus solver requirements [21]), there is a need to determine both Young's modulus and the plot of true stress vs plastic strain. This plot is presented in **Fig. 2**. The results of material investigations showed that S185 steel has Young's modulus of 209 600 MPa, yield stress value of 163 MPa and ultimate tensile strength (UTS) of 304 MPa.

During experimental investigations, 8 specimens (joints) were prepared. The results of tension tests of these joints showed that the average value of destructive force was equal to 5282 N. Quantitative results of experimental investigations of the joint showed that the permanent deformations occur in adherend. This deformation was visible after fracture of the joint (**Fig. 3**).

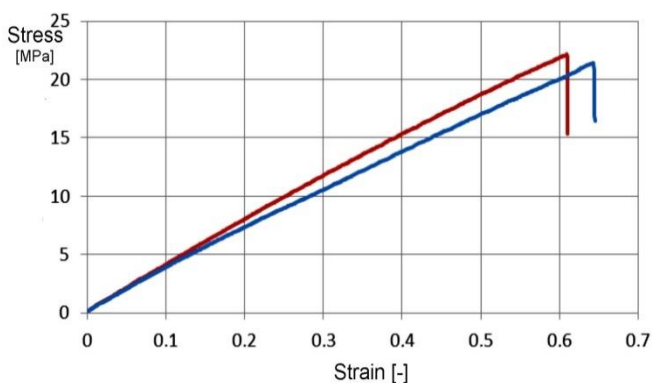


Fig. 1 Stress-strain characteristics for Araldite 2014-1 adhesive after hardening

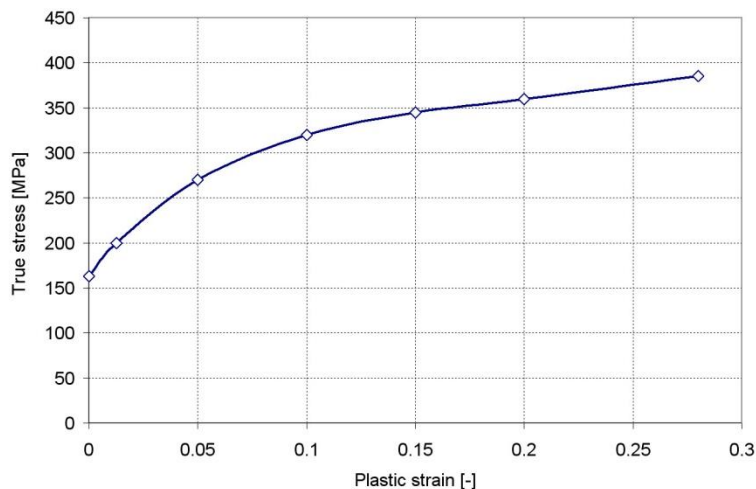


Fig. 2 Plot of true stress vs plastic strain for S185 steel used for definition of elastic-plastic model of adherend material

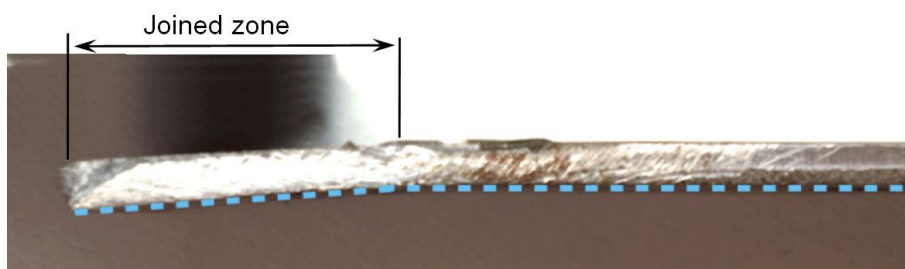


Fig. 3 A segment of the adhesive joint after the destructive test. The permanent deformation of adherend is visible

3 Numerical model of joint, the load and boundary conditions

The joint was composed of two sheets (dimensions: $2 \times 25 \times 100$ mm) made from S185 low-carbon steel (**Fig. 4**). The sheets were adhesively bonded using Araldite 2014-1 epoxy adhesive. The thickness of the adhesive layer is equal to 0.2 mm. The adhesive was modelled as linear-elastic material (on the base of the result presented in **Fig. 1**). On the corner of the adhesive layer, the radius ($R = 0.05$ mm) was defined (**Fig. 5**). The value of this radius was obtained during measuring the joint geometry using an optical microscope. The joint was loaded by the force $F = 5282$ N (destructive force of joint obtained from experimental investigations). In this study, two models of adherend material were considered (linear-elastic and elastic-plastic).

The numerical model of the joint is composed of 134 589 QUAD-8 finite elements (with second-order shape function [21]) and 406 706 nodes. The finite element mesh was concentrated in the border zone of the adhesive layer. The plain strain numerical analysis was considered in order to determine the stress state in a central section of the joint. The simplification of analysis to plain strain decreases the size of the numerical task. The set of nodes located on the left part of the joint (**Fig. 4**) was constrained (translations: $T_x = 0$, $T_y = 0$). For nodes located in the right part of the joint the partial fixation was defined ($T_y = 0$). These boundary conditions are

equivalent to the conditions occurring in experimental tension test of the joint. The force $F = 5282$ N was defined on right border surface of the model (**Fig. 4**).

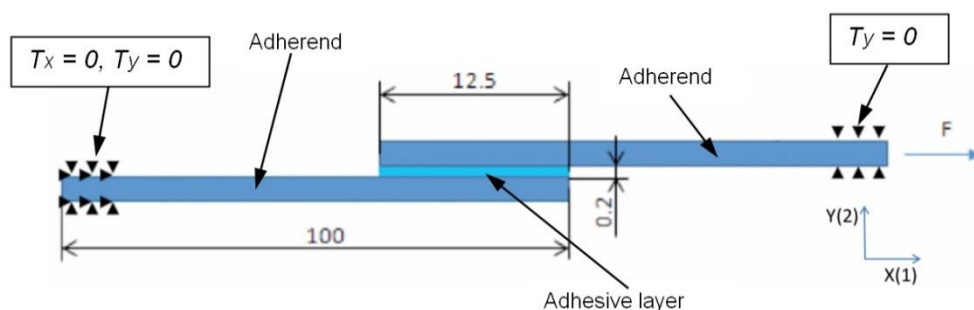


Fig. 4 Dimensions, boundary conditions and load of joint

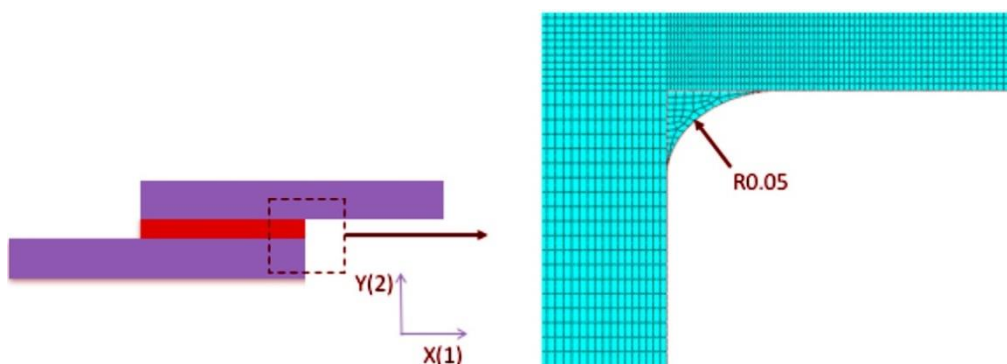


Fig. 5 Radius $R = 0.05$ mm defined for the corner of the adhesive layer

4 Stress and strain analysis of adhesive joint

As a result of numerical computations using a finite element method the stress and strain distributions were obtained for the single lap adhesive joints, for two following configurations:

- Linear-elastic model of S185 steel (adherend material), described by Young's modulus (209.6 MPa) and the Poisson's ratio (0.3), linear analysis.
- Elastic-plastic model of S185 steel (adherend material), described by Young's modulus and the true stress vs plastic strain plot (**Fig. 2**), nonlinear analysis.

In **Fig. 6** the stress distribution for the joint with a linear-elastic model of adherend material is presented. As seen in this figure, the largest equivalent stress (calculated for destructive force $F = 5282$ N) has a value of 473.42 MPa. The largest stress area occurs in the sheets, just near the end of the adhesive layer. Obtained results show that equivalent stress is about 3 times larger than the yield stress of S185 steel (163 MPa). It can be concluded that the stress distribution computed for considered joint (with a linear-elastic model of adherend material) could be not real.

In **Fig. 7** the result of nonlinear stress analysis of joint with an elastic-plastic model of adherend material was presented. The assumption of the elastic-plastic model of adherend material caused that the maximum equivalent stress (according to Huber-Mises-Hencky criterion) in the sheets was reduced to the value of about 230 MPa (**Fig. 7**). This value exceeds the yield stress of S185

steel. It means that during the plastic deformation of adherend the material was strengthened. The zone of maximum stress area is located on the surface of the sheet, near the end of the adhesive layer. As can be seen in **Fig. 7**, the complex stress state occurs in the joint. The sheets were subjected to both the tension and the bending (related to the non-axial load of the lap joint). Magnification of the border (adherend-adhesive) zone of the joint is presented in **Fig. 8**. After plasticization of the adherend, the bending state increased what causes larger deformation of the joint.

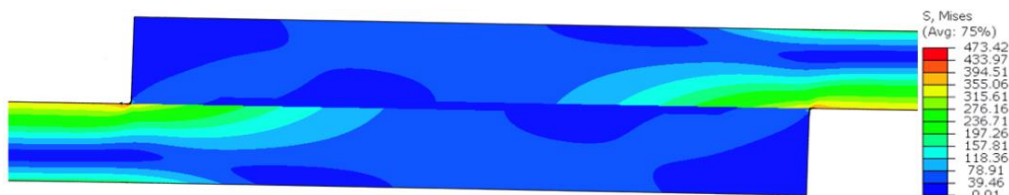


Fig. 6 Equivalent stress distribution (according to Huber-Mises-Hencky criterion) for central part of the joint (linear-elastic model of adherend material, linear analysis, $F = 5282$ N)

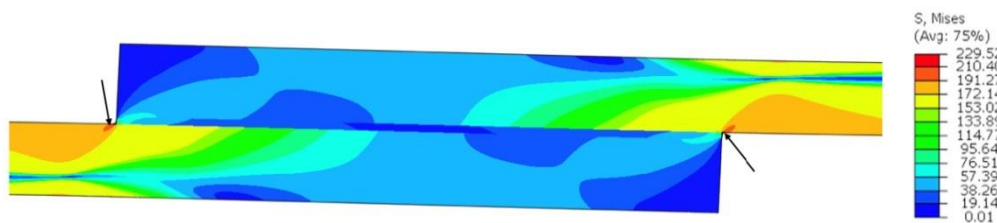


Fig. 7 Equivalent stress distribution (according to Huber-Mises-Hencky criterion) for central part of the joint (elastic-plastic model of adherend material, nonlinear analysis, load $F = 5282$ N)

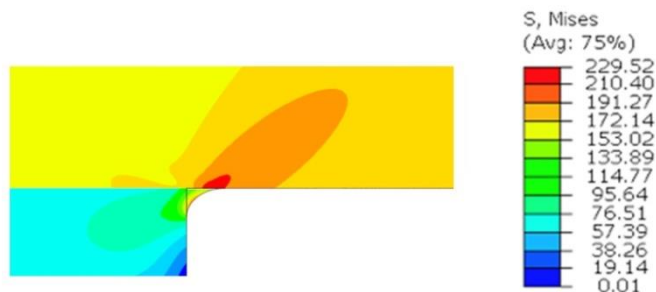


Fig. 8 Stress distribution in magnified adherend-adhesive zone of the joint

In **Fig. 9** the distribution of the plastic strain magnitude in adherend was presented. It is visible in this figure that during loading of the joint by destructive force ($F = 5282$ N) the plastic strain area achieves more than 50% of the sheet cross-section area. The largest plastic strain zones (points A1, **Fig. 9**) are located on the sheet surface. The plastic strain zones begin in sheets, on the border of the adherend-adhesive layer (points B1).

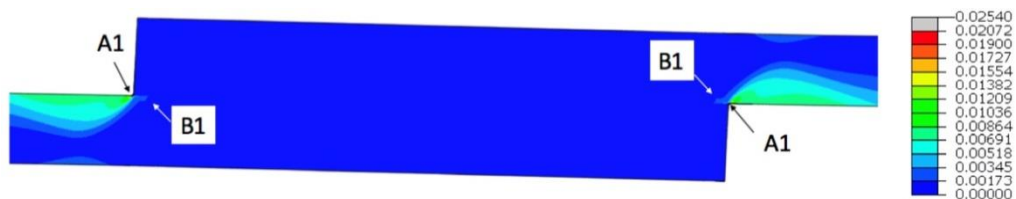


Fig. 9 Plastic strain distribution in the joint loaded by destructive force ($F = 5282 \text{ N}$)

5 Analysis of stress in adhesive layer

Presented above results were related to the stress in the sheets (adherents). Detailed analysis of the stress in the adhesive layer will be presented in the next part of this study. The adhesive layer of the joint loaded by destructive force the maximum principal (σ_1) stress has a value of about 244 MPa (**Fig. 10**). The zone of maximum stress is located on the radius of the adhesive layer. The maximum tearing (S22) stress has a value of 222.14 MPa (**Fig. 11**).

In **Fig. 12** the joint section is presented. In this figure, the X-axis is located in the adhesive layer, at a distance of 0.02 mm from the adhesive-adherend border. The X-axis location was defined on the base of experimental results (the cohesive fracture of the adhesive layer was located at a distance of 0.02 mm from the adhesive-adherend border). The stress components used in the description of the results of a finite element method computations are presented in **Fig. 13**.



Fig. 10 Maximum principal stress distribution in the adhesive layer ($F = 5282 \text{ N}$, elastic-plastic model of adherend)



Fig. 11 Tearing S22 stress distribution in the adhesive layer of joint ($F = 5282 \text{ N}$, elastic-plastic model of adherend)

Results presented in **Fig. 14** show that in the left part of the adhesive layer the tearing stress (S22) has the following values: 52 MPa for a linear-elastic model of adherend material, and 58 MPa for elastic-plastic material. The maximum value of tearing stress appeared on the right side of the adhesive layer. Value of S22 stress (for a linear-elastic model of adherend material) is

equal to 105 MPa. After the definition of adherend material as elastic-plastic, the S22 stress in the adhesive layer increases to the value of 135 MPa (**Fig. 14**).

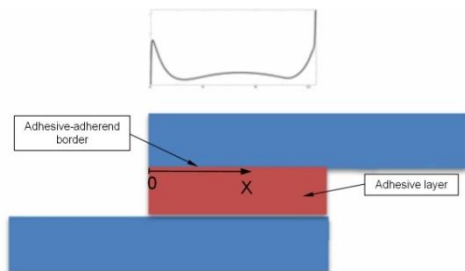


Fig. 12 Location of X-axis used for the description of the horizontal axis of plot presented in **Fig. 14**

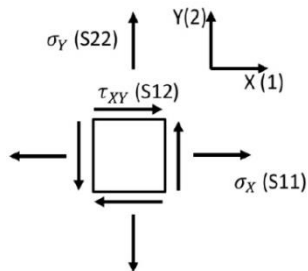


Fig. 13 Description of stress components (S12 – shear stress, S22- tearing stress)

The materials of sheets were considered (in the second case) as elastic-plastic. From this reason, in this work, the nonlinear static analysis was used [21]. In computations the load $F = 5282$ N was divided into smaller increments. In the analysis, the constant increment (step time) of 0.1 was defined. As a result of computations (for first increment, step time of 0.1) the stress state was obtained for the load which is equal to 10% of the destructive force. During next increments, the load is increased. The analysis is finished if the step time equals 1.

In **Fig. 15** the maximum shear stress values in the adhesive layer as a function of step time is presented. Step time value of 1 should be related to the force of $F = 5282$ N. For the linear-elastic material of adherend a linear increase of shear stress in the adhesive layer is observed (**Fig. 15**). The different character has a curve defined for an elastic-plastic model of adherend material. In this case, the stress in the adhesive layer is proportional to the load, to the step time of 0.5 only. At higher values of step time, the progressive increase of stress is observed. It means that the first plastic strain occurs in adherend (made out of S185 steel) at a load of 2641 N which is equivalent to 50% of the joint destructive force.

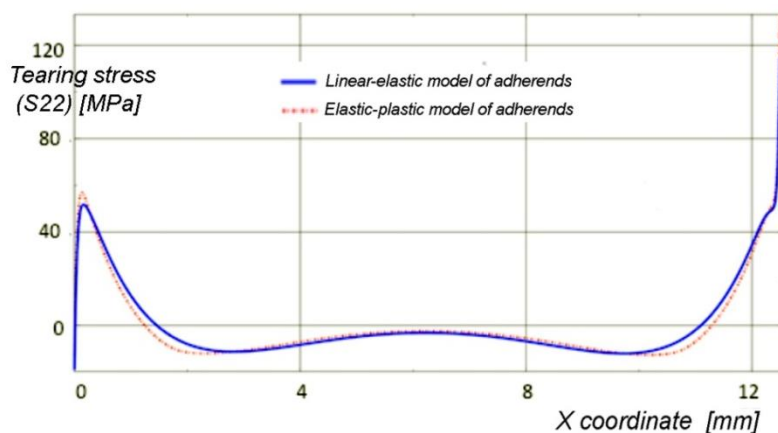


Fig. 14 Tearing stress values as a function of X-coordinate in the adhesive layer for linear-elastic and elastic-plastic model of adherend material ($F = 5282$ N)

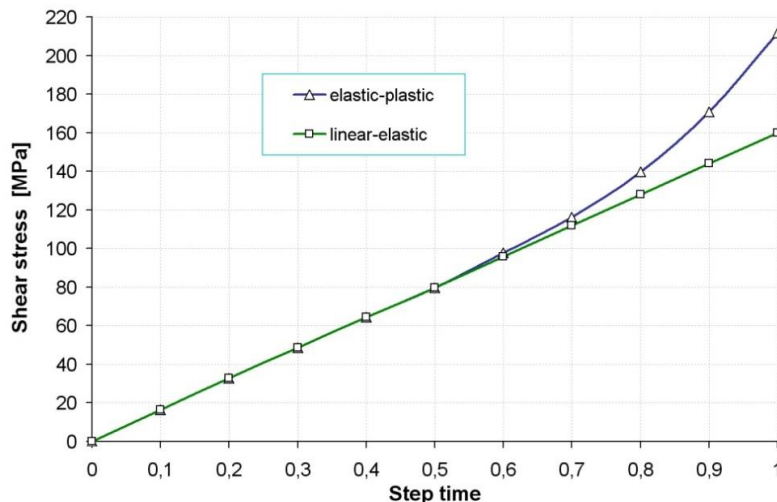


Fig. 15 Maximum values of shear stress (S12) in the adhesive layer as a function of step time. Step time of 1 is equal to destructive force

6 Conclusions

In this work, the results of stress and strain analysis of adhesive lap joint were presented. In this analysis, the linear-elastic and the elastic-plastic models of material were defined for an adherend. As a result of numerical finite element analysis, both the plastic strain and the stress distributions were obtained for the joint components. In next part of the study, the tearing stress (S22) in the adhesive layer as a function of step time was specified. The maximum Huber-Mises stress in joined sheets is equal to 473 MPa (for a linear-elastic model of adherend material). This value of stress exceeds about 3 times the yield stress of S185 steel. Into joint with an elastic-plastic model of joined material, the maximum Huber-Mises stress in the sheets achieves about 230 MPa. The plastic deformation of adherend material causes larger distortion of sheets in the area close to the edge of an adhesive layer. Results of performed work showed that at loads larger than 50%-60% of destructive force a sudden increase of stress is observed in the adhesive layer. In the presented case, the use of an elastic-plastic model of adherend material caused an increase of the maximum stress in the adhesive layer at about: 37% (σ_1), 24% (tearing stress, S22) and 31% (shear stress, S12) in comparison to the joint with a linear-elastic model of joined material. In joints of materials with a low yield stress, the elastic-plastic model of joined materials should be used in order to correct both the stress and the strain estimation into the adhesive layer.

References

- [1] K. Biruk-Urban., J., Kuczmaszewski: *Technologia i Automatyizacja Montażu*, Vol. 2, 2013, p. 31-35
- [2] E.M. Petrie: *Handbook of Adhesives and Sealants*, McGraw - Hill Professional, New York, 2006
- [3] G. Habenicht.: *Kleben erfolgreich und fehlerfrei: Handwerk, Praktiker, Ausbildung, Industrie*, Wiesbaden, Vieweg +Teubner, 2008
- [4] G. Habenicht: *Kleben - Grundlagen, Technologien, Anwendungen*, Springer, Berlin, 2008

- [5] A.V. Pocius: Adhesion and Adhesives Technology: *An Introduction*, Cincinnati Carl Hanser Verlag GmbH Co KG, 2012
- [6] Verein Deutscher Ingenieure: VDI 2229 Metallkleben, *Metallkleben Hinweise für die Konstruktion und Fertigung*, VDI-Gesellschaft für Konstruktion und Entwicklung, 1979
- [7] J. Kuczmaszewski: *Fundamentals of metal-metal adhesive joint design*, Lublin University of Technology, Polish Academy of Sciences, Lublin, 2006
- [8] Z.M. Yana, Y. Moua, X.Y. Yib, X.L. Zhenga, Z. Lia: International Journal of Adhesion & Adhesives, Vol. 27, 2007, p. 687–695, doi: 10.1016/j.ijadhadh.2007.02.003
- [9] I. Pires, L. Quintino, J.F. Durodola, A. Beevers: International Journal of Adhesion & Adhesives, Vol. 23, 2003, p. 215–223, doi: 10.1016/S0143-7496(03)00024-1
- [10] J. Godzimirski, S. Tkaczuk, R. Marek: *Strength of adhesive joints*, Warsaw, 2009
- [11] H. Xiacong: International Journal of Adhesion & Adhesives, Vol. 31, 2011, p. 248-264, doi: 10.1016/j.ijadhadh.2011.01.006
- [12] L. Witek: Key Engineering Materials, Vol. 598, 2014, p. 261-268, DOI: 10.4028/www.scientific.net/KEM.598.261
- [13] Y. Hua, L. Gu, M. Trogdon: International Journal of Adhesion & Adhesives, Vol. 38, 2012, p. 25-30, DOI: 10.1016/j.ijadhadh.2012.06.003
- [14] L. Witek: Engineering Failure Analysis, Vol. 66, 2016, p. 154-165 DOI: 10.1016/j.engfailanal.2016.04.022
- [15] K. Zielecki L. Witek: *Influence of young modulus of connected materials on ultimate strength of beveled adhesive joints*, Proceedings of International Conference „Advances in Micromechanics of Materials”, Rzeszów, 2014
- [16] L. Witek: Key Engineering Materials, Vol. 598, 2014, p. 269-274, DOI: 10.4028/www.scientific.net/KEM.598.269
- [17] Y. Boutar, S. Naïmi, S. Mezlini, L. F.M. da Silva, M. B. S. Ali: Engineering Fracture Mechanics Vol. 177, 2017, p. 45-60, DOI: 10.1016/j.engfracmech.2017.03.044
- [18] L. Witek: Engineering Failure Analysis, Vol. 49, 2015, p. 57-66, doi: 10.1016/j.engfailanal.2014.12.004
- [19] K. Zielecki, L. Witek, F. Stachowicz: Mechanika, Vol. 89 No. 2/17, 2017, p.121-130, DOI: 10.7862/rm.2017.22
- [20] http://www.salzgitterstahlhandel.pl/pl/produkty/gatunki_normy/gatunki_EN10025
- [21] ABAQUS User's Manual, Abaqus Inc., 2009

Acknowledgements

The research leading to these results has received funding from the People Programme (Marie Curie International Research Staff Exchange) of the European Union's Seventh Framework Programme FP7/2007-2013/ under REA grant: PIRSES-GA-2013-610547.